RSC Advances

PAPER

View Article Online
View Journal | View Issue

Cite this: *RSC Adv.*, 2021, **11**, 24543

Experimental and molecular dynamics study into the surfactant effect upon coal wettability

Yi-ting Liu,[a] Hong-mei Li,*[ac] Ming-zhong Gao,[ab] Si-qi Ye,[a] Yun Zhao,[c] Jing Xie,[a] Gui-kang Liu,[a] Jun-jun Liu,[a] Lu-Ming Li,[c] Jie Deng[c] and Wei-Qi Zhou[c]

Received 10th March 2021
Accepted 23rd June 2021

DOI: 10.1039/d1ra01882e

rsc.li/rsc-advances

In order to improve the wettability and permeability of coal seams, the water injection efficiency of coal seams has to be boosted, the amount of dust generation has to be reduced, and coal and gas outburst must be prevented, and a surfactant is used to modulate the coal surface wettability. In this work, taking coal samples from Pingdingshan mine in Henan as the research object, their surface chemistry was initially scrutinized and then coal surface engineering *via* surfactants was inspected by a contact angle test. The coal wettability was ameliorated with surfactants, particularly using the 1 wt% non-ionic surfactant Triton X-100, which elicited a 47% lower contact angle than the raw coal. The surface free energy of the coal sample modified by 1.0 wt% Triton X-100 was increased from 44.51 mN m^{-1} to 49.52 mN m^{-1}. The microstructural characteristics of coal samples allowed leveraging the Wiser model to construct three kinds of surfactant-coal adsorption models to dissect the adsorption configuration of the system. The results indicate that the addition of surfactants increases both the interaction of water with the coal and the diffusion coefficient of water molecules, resulting in the coal surface transformation from hydrophobicity to hydrophilicity. Our current work can provide salutary guidance and reference for coal water injection and dust suppression.

Introduction

Coal seams feature dense structures, poor hydrophilicity and permeability, and hence, coal mining often causes a cascade of serious disasters such as dust pollution, coal and gas outburst, and gas explosion.[1–4] The traditional coal seam water injection method embarrasses both water diffusion on the coal surface and uniform wetting of coal due to the low free energy of coal body. To overcome the limitation and low efficiency of physical ways, chemical strategies emerge to boost the coal wettability.[5] Surfactants have a unique amphiphilic structure. Their hydrophobic group can be adsorbed on the low energy surface to form an adsorption layer and the hydrophilic group faces the water phase, thus changing the wettability of the hydrophobic surface.[6–11] Crawford *et al.*[9] studied the surfactant effect on the surface properties of different coals and found that surfactants can significantly augment the coal's wetting effect. Kang Jianting[12] revealed that both inorganic electrolyte (sodium sulfate) and anionic surfactant (sodium dodecyl sulfate, SDS) can chemically decorate the anthracite surface groups to foster hydrophilicity. Ni Guanhua[13] *et al.* piggybacked on both the contact angle test and Fourier transform infrared spectroscopy to disclose that incorporation of NaCl into an anionic surfactant (SDS) can notably tweak the functional groups of the coal dust surface and wettability. Therefore, surfactants can promote the wettability/permeability of the coal surface, and thus the coal seam infusion, reducing the dust generation. The adsorption characteristics of water and surfactants on the coal surface can be untangled by molecular dynamics simulation. Nie Baisheng *et al.*[14] applied molecular thermodynamics and surface physical chemistry theory to analyze the coal surface free energy landscape and the micromechanism of coal adsorbing water, and discuss the wetting effect of surfactant on coals. The data signify that water molecules and the coal surface can strongly interact *via* intermolecular forces and hydrogen bonds. Paria *et al.*[15] delved into the surfactant adsorption process on the hydrophilic solid–liquid interface and unravelled the dependence of the kinetics and equilibrium adsorption of the surfactant types on the surfactant properties and solid surface. Yangchao Xia *et al.*[16] studied the impact of cationic surfactants (dodecyl trimethylammonium bromide, DTAB) on the flotation of low-rank coals using an oil-based collector (dodecane) by combining the experimental test and molecular dynamics simulation. The simulation results well tally with the experimental conclusions. The NPEO-10 adsorption behavior on the sub-bituminous coal model surface from molecular dynamic stimulation by Xiaofang You *et al.*[17] articulated that the raised hydrophobicity endowed by NPEO-10 underlies the robust repelling of water molecules by coal surfaces. Yuan Mingyue *et al.*[18] studied the micro dynamic process of wetting and adsorption of fatty alcohol

[a]*State Key Lab of Hydraulics and Mountain River Engineering, College of Water Resource & Hydropower, Sichuan University, Chengdu, Sichuan 610065, China*
[b]*Guangdong Provincial Key Laboratory of Deep Earth Sciences, Geothermal Energy Exploitation and Utilization, College of Civil and Transportation Engineering, Shenzhen University, Shenzhen 518060, China*
[c]*College of Food and Bioengineering, Chengdu University, Chengdu, Sichuan 610106, China*

polyoxyethylene ether-9 on lignite by molecular dynamics simulation and experimental measurement. However, most of the above surfactant adsorption models are based on low-rank coal molecules, which are not suitable for bituminous coals with high degree of coalification and poor hydrophilicity. To molecularly study the surfactant adsorption at the water–coal interface, a suitable coal macromolecular structure model is necessitated to increase the simulation calculation accuracy. Despite the complexity of the coal macromolecule structure, its surface functional groups can be identified by FT-IR spectroscopy. For example, Zhou *et al.*[19] uncovered more hydrophobic groups and fewer hydrophilic groups on the low-ash coal samples by infrared spectroscopic analysis of the functional groups of the oxidized coal. A portfolio of elemental analysis, nuclear magnetic carbon spectrum, infrared spectrum and other tests by Lu Youzhi *et al.*[20] enables establishing a molecular structure model of oxidized lignite with an aromatic ring mainly connected by oxygen-containing functional groups.

The previous experiments and molecular simulation of the surfactant-modified coals mostly use ionic surfactants and lack the systematic comparison of the surfactant-type effects. In this work, experimental and molecular dynamic investigation into the surface chemistry of Pingdingshan Coal Group D in Henan Province was executed. Three kinds of surfactants were selected to modify the coal surface structure to effectively modulate the wettability. The surface free energy and solid–liquid interface interaction energy were calculated. According to the characteristics of surface functional groups of coal molecules, a model of surfactant adsorption on coals was established. Molecular dynamics study simulates the adsorption motifs of different surfactants on coal surfaces and clarifies the modification law.

Materials and methods

Sample preparation

The coal samples used in the experiment were taken from Group D of Pingdingshan Coal Mine in Henan Province. The coal samples were first collected according to the international standard and then sealed immediately to prevent pollution and oxidation. The samples were grinded by ball mill at 870 speed for 30 minutes, sieved with 200 mesh (mesh diameter of 75 μm), and stored in sample bags for FT-IR.

By preliminary experiments, three kinds of surfactants with good wettability, namely, SDBS (anionic surfactant), JFC (nonionic surfactant) and Triton X-100 (nonionic surfactant) were selected. To explore the influence of surfactant concentrations on the modification effect of coals, ten mass fraction gradients (0.1–1.0 wt%) of each surfactant were compared. The molecular formula and structure of the selected surfactant are shown in Table 1.

The coal samples were soaked in a surfactant-containing aqueous solution for 24 hours, taken out, filtered, and finally dried at 60 °C for 12 hours. The contact angle of the treated coal samples was tested.

Experimental methods

The surface functional groups of coal samples were determined using a Nicolet 6700 Fourier transform infrared spectrometer. The pulverized coal was first mixed with KBr in a 100/1 mass ratio and subsequently made into transparent thin sheets with a thickness of 0.1–1.0 mm and a diameter of 13 mm. The test range was 4000–400 cm^{-1}.

The contact angle between coal and distilled water, formamide, and diiodomethane droplets was measured using a JC2000D1 contact angle measuring instrument. Each group containing identical pulverized coals was pressed into a thin sheet with a diameter of 1 cm and a thickness of 1 mm. To avoid large errors caused by other factors, it was assumed that the contact angle of the coal sample moving upward to contact the droplet took 0 s, and the contact angle of the coal sample moving down for 1 s was taken as the measured value. Each group of coal samples was pressed into 3 pieces, each piece was measured 5 times, and finally, the average value was taken to calculate the contact angle. All of the contact angle tests were carried out at the same temperature ((25 ± 1) °C). The allowable error of contact angle measurement was 0.1°.

Results and discussion

FT-IR analysis

The organic matter on the coal surface is composed of structural units with various polar functional groups, whose type and

Table 1 Surfactants used in the test

Surfactant	Molecular formula	Purity	Molecular structure
SDBS	$C_{18}H_{29}NaO_3S$	Analytically pure	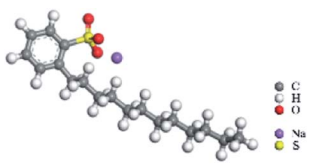
JFC	$C_{17}H_{36}O_6$	Chemical pure	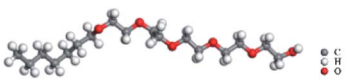
Triton X-100	$C_{34}H_{62}O_{11}$	Analytically pure	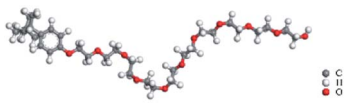

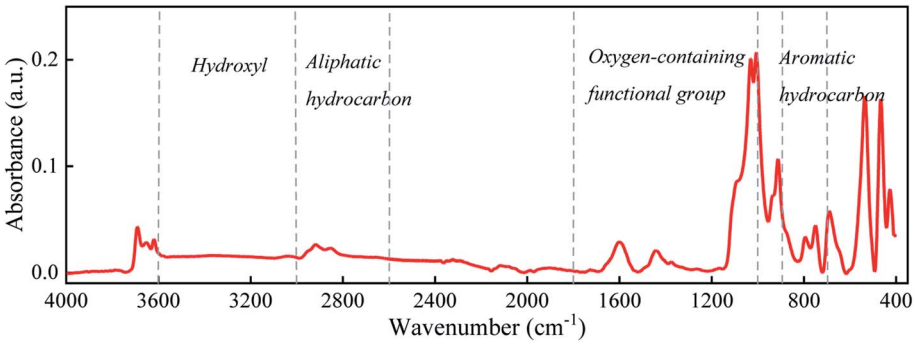

Fig. 1 Infrared spectrum of raw coal.

quantity can be described by the infrared spectrum. As the molecular structure of coal is complex, and includes a wide variety of groups, multi-peak overlapping occurs in the infrared spectrum. Thus, the infrared spectrum of coal (Fig. 1) is judiciously divided into four sections: hydroxyl (3700–3000 cm^{-1}), aliphatic hydrocarbon (3000–2600 cm^{-1}), oxygen-containing functional group (1800–1000 cm^{-1}) and aromatic hydrocarbon (900–700 cm^{-1}) for peak fitting.[21–23] After the baseline correction, the Gaussian distribution function was selected for peak fitting, and the outcomes are depicted in Fig. 2 and Table 2.

The main functional groups and bonding types in the range of 3000–3600 cm^{-1} are hydroxyl groups and hydrogen bonds. The hydrogen bond structure produced by free water molecules or other parts of the coal structure affects the absorption of infrared light, and the absorption peaks of this range become wider and slower. The absorption peak near 3400 cm^{-1} belongs to the stretching vibration of phenol, alcohol, carboxylic acid, peroxide and hydroxyl groups in water, indicating a certain amount of associated hydroxyl groups on coal surfaces. The hydroxyl groups are the main adsorption sites of water

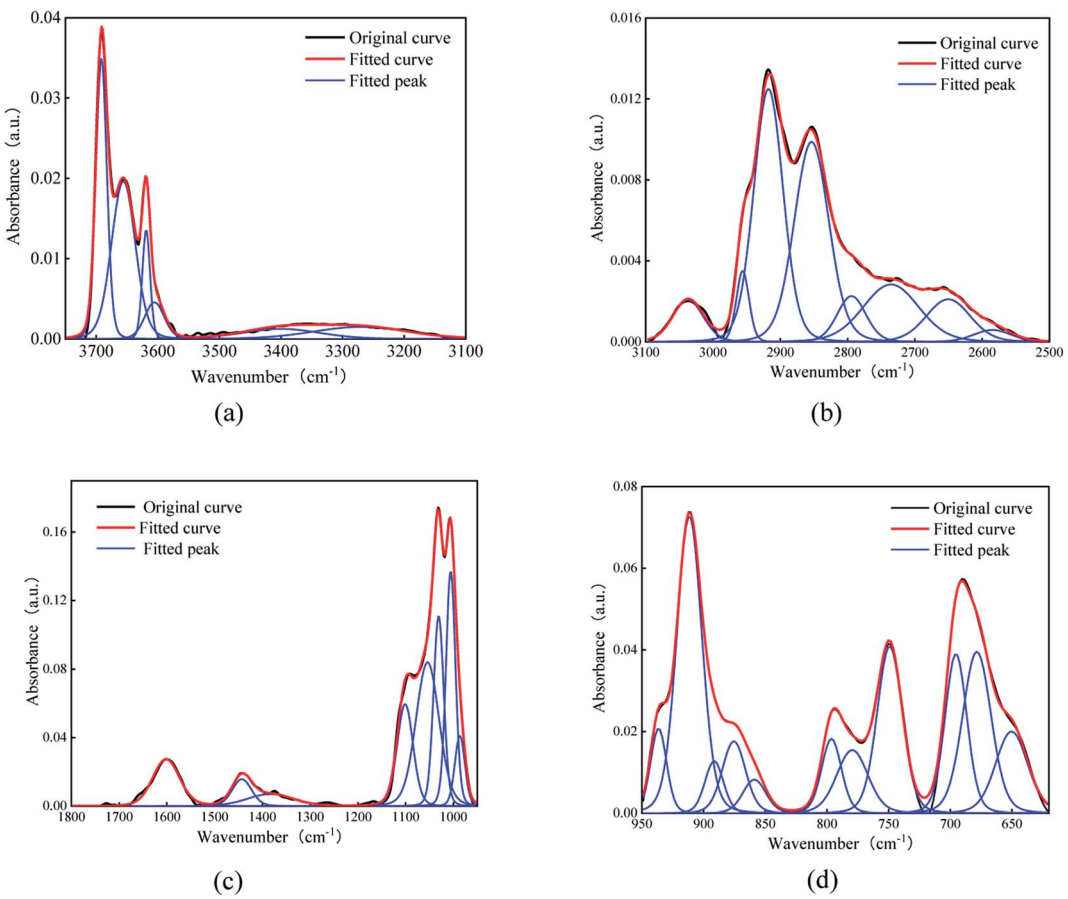

Fig. 2 Peak fitting results of infrared spectra. (a) hydroxyl, (b) aliphatic hydrocarbons, (c) oxygen-containing functional groups, (d) aromatic hydrocarbon.

Table 2 A summary of the fitting data of infrared spectra

Functional groups	Number	Peak position	Relative peak height	Area of relative integration	Functional groups	Number	Peak position	Relative peak height	Area of relative integration
Hydrocarbon	1	3691	0.0352	0.8118	Aliphatic hydrocarbon	1	3036	0.0020	0.1229
	2	3655	0.0196	0.9934		2	2955	0.0035	0.0869
	3	3618	0.0134	0.2237		3	2917	0.0123	0.7131
	4	3605	0.0045	0.1899		4	2853	0.0098	0.6656
	5	3400	0.0016	0.2061		5	2794	0.0022	0.1264
	6	3270	0.0016	0.3013		6	2735	0.0028	0.3084
Aromatic	1	936	0.0205	0.3504		7	2650	0.0021	0.1809
hydrocarbon	2	911	0.0736	1.9224		8	2584	0.0006	0.0433
	3	891	0.0127	0.2485	Oxygen-containing	1	1601	0.0273	2.0124
	4	875	0.0176	0.4331	functional groups	2	1442	0.019	0.8308
	5	858	0.0081	0.1991		3	1383	0.0086	0.8742
	6	796	0.0181	0.3816		4	1101	0.0595	2.5846
	7	779	0.0154	0.5101		5	1054	0.0839	5.3225
	8	749	0.0414	1.0865		6	1030	0.1106	3.0944
	9	695	0.0388	0.9054		7	1005	0.1362	3.5624
	10	678	0.0395	1.1939		8	986	0.0408	1.1272
	11	650	0.0199	0.6774					

molecules, which is an important factor affecting the wettability of the coal surface.

The stretching vibration of aliphatic hydrocarbon varies between 2600 and 3000 cm^{-1}. The peaks from 3030 cm^{-1} to 2850 cm^{-1} represent the breathing vibration of the aromatic methylene group, antisymmetric stretching vibration of the methyl group, antisymmetric stretching vibration of the methylene group and symmetric stretching vibration of the methylene group, whose ratio sequentially accounts for 1.22 : 0.87 : 7.13 : 6.65. The peak area reflects the proportion of each species. Thus, the methylene structure in Group D coal heavily outnumbers the methyl group, and the symmetric stretching vibration of methylene is stronger than its antisymmetric mode, further elucidating that aliphatic hydrocarbons in Group D coal mainly exist as long-chain alkanes. The absorption peak near 2560 cm^{-1} deals with the stretching vibration of the sulfhydryl group, whose polarity is weaker than that of the hydroxyl group.

The band at 1800–1000 cm^{-1} is primarily assigned to the stretching vibration of oxygen-containing functional groups. The stretching vibration of the carboxyl group emerge as a weak peak around 1700 cm^{-1}, presenting a relatively low carboxyl group content. The absorption peaks near 1600, 1110, 1050, and 1035 cm^{-1} are ascribed to the stretching vibration of –C=C– in aromatic hydrocarbon, S=O stretching vibration, Si–O–Si or Si–O–C, and C–O aliphatic ether bond, respectively. Hence, in addition to hydroxyl and carboxyl groups, the oxygen-containing functional groups in coal comprise largely silicon ether bonds and aliphatic ether bonds. The deformation vibration of aromatic hydrocarbon exists near 900–700 cm^{-1}. The strong and narrow absorption signal near 950 cm^{-1} typifies the bending vibration of –OH in carboxylic acid. The one around 870 cm^{-1}, 800 cm^{-1} and 750 cm^{-1} holds accountable for the out-of-plane deformation vibration of –CH in monosubstituted aromatic hydrocarbons, ortho trisubstituted aromatic hydrocarbons and penta-substituted aromatic hydrocarbons, respectively, with their ordinal ratio being 0.43 : 0.38 : 1.08.

Our infrared spectra data alongside prior studies testify that the basic motif of the coal molecule is the aromatic condensation structure, and the oxygen-containing functional groups, aliphatic hydrocarbons, and sulfur-containing functional groups constitute its side branch chain. The surficial oxygen-containing functional groups are usually hydrophilic and tend to form hydrogen bonds with polar water molecules, while the main aromatic structure and aliphatic hydrocarbon side chain have weak attraction to water molecules and thus are hydrophobic. This answers for the poor hydrophilicity of the coal surface.

Contact angle test

The contact angle θ is the angle from the solid–liquid interface to the gas–liquid interface at the junction of the solid, liquid and gas phases of the liquid droplet on the solid surface. According to Young's equation,[24] the contact angle θ has the

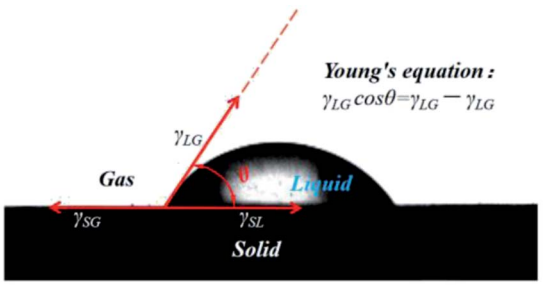

Fig. 3 Contact angle and Young's equation.

following relation with the interfacial tension of solid/gas(γ_{SG}), solid/liquid (γ_{SL}) and liquid/gas (γ_{LG}) interfaces (Fig. 3):

$$\gamma_{LG}\cos\theta = \gamma_{SG} - \gamma_{SL} \quad (1)$$

Therefore, the contact angle can act as a crucial criterion to assess the affinity between liquid molecules and the solid surface, namely, the wetting effect.[25] The stronger the affinity, the easier the spread on the solid surface, the smaller the contact angle. This affinity is determined by the liquid–solid surface properties.

The contact angle test results show that the contact angle of coal soaked in distilled water is 84.924°, which indicates that untreated raw coal has poor hydrophilicity and low surface free energy, and pure water is difficult to spread on the coal surface. The contact angle decreases with the increment in surfactant concentration from 0.1 to 1.0 wt%, unfolding the ameliorated coal surface free energy and hydrophilicity by surfactants and so the easier wetting of coal by pure water. This is because that there are many vacant adsorption sites on the coal surface, surfactants are adsorbed on the coal surface, and hydrophilic molecular chain covers the hydrophobic part of the coal surface, which increases the attraction of coal surface to water. The growing surfactant concentration triggers off adsorption of the more surfactant molecules on the coal surfaces. Clearly, a 0.1–1.0 wt% dosage will stage no saturated surfactant adsorption and hence a monolayer adsorption on the coal surface. Fig. 4 evidences that, among the three surfactants, Triton X-100 has the best modification effect, with a 44.9° contact angle at 1.0 wt%, 47% lower than that of raw coal. The modification effect increases in the following sequence: Triton X-100 > SDBS > JFC.

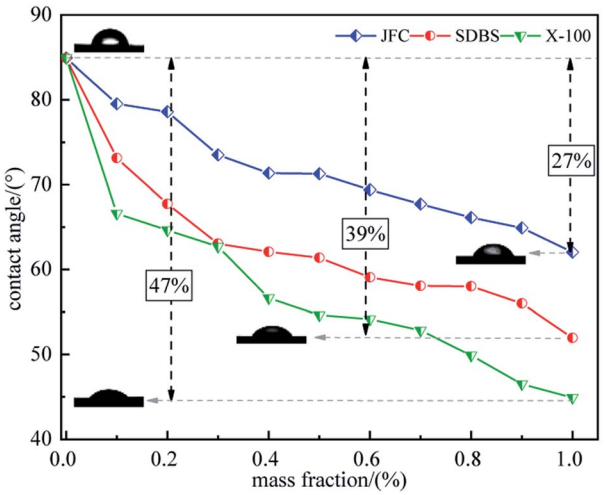

Fig. 4 Contact angle test results.

Table 3 Physical parameters of test liquids

	Surface free energy component/(mN m^{-1})			
Test liquid	γ_l^{LW}	γ_l^+	γ_l^-	γ_l
Distilled water	21.8	25.5	25.5	72.8
Formamide	39	2.28	39	57.4
Diiodomethane	50.8	0	0	50.8

In order to further explore the change in surface properties of coal samples modified by surfactants, the van Oss–Chaudhury–Good theory was used to calculate the surface free energy and solid–liquid interface interaction energy of coal. According to the van Oss–Chaudhury–Good theory, the total surface free energy was calculated γ. It consists of two parts: non-polar part γ^{LW} (*i.e.*, dispersion force) and polar part γ^{AB} (*i.e.*, Lewis acid–base).[26,27] The non-polar component is mainly Lifshitz–van der Waals, while the polar component (Lewis acid–base interaction) is mainly hydrogen bond and electron donor and acceptor γ^- and γ^+.[28,29] The surface free energy of the solid γ_s can be calculated as follows:

$$\gamma_s = \gamma_s^{LW} + \gamma_s^{AB} = \gamma_s^{LW} + 2\sqrt{(\gamma_s^+\gamma_s^-)} \quad (2)$$

where γ_{sl} is the total surface free energy of the solid, γ_s^{LW} is the non-polar Lifshitz–van der Waals interaction on the solid surface, γ_s^{AB} is the polar Lewis acid–base interaction on the solid surface, and γ_s^- and γ_s^+ are the Lewis acid–base interaction on the solid surface, respectively. The free energy between the solid and liquid interface is expressed by the following formula (3):

$$\gamma_{sl} = \gamma_s + \gamma_l - 2\left(\sqrt{\gamma_s^{LW}\gamma_l^{LW}} + \sqrt{\gamma_s^+\gamma_l^-} + \sqrt{\gamma_s^-\gamma_l^+}\right) \quad (3)$$

Among them, γ_{sl} is the free energy between the solid and liquid interface, γ_l is the total surface free energy of liquid, γ_l^{LW} is the non-polar Lifshitz–van der Waals interaction of liquid surface, and γ_l^- and γ_l^+ are the Lewis acid–base interaction of the liquid surface respectively. According to Young's equation:

Table 4 Surface free energy of raw coal

	Contact angle/(°)			Surface free energy component/(mN m^{-1})			
Sample	Distilled water	Formamide	Diiodomethane	γ_s^{LW}	γ_s^+	γ_s^-	γ_s
Coal	84.9	46.8	33.0	42.94	1.00	0.62	44.51

$$\gamma_s = \gamma_{sl} + \gamma_l \cos\theta \quad (4)$$

$$\gamma_{sl} = \gamma_s^{+}\gamma_s^{-} - W_a \quad (5)$$

$$W_a = \gamma_l(1+\cos\theta) = 2\left(\sqrt{\gamma_s^{LW}\gamma_l^{LW}} + \sqrt{\gamma_s^{+}\gamma_l^{-}} + \sqrt{\gamma_s^{-}\gamma_l^{+}}\right) \quad (6)$$

W_a is the adhesion work and θ is the contact angle. By combining formula (2)–(5), formula (6) was obtained as follows:

Furthermore, the interaction energy between deionized water and coal can be calculated. The solid–liquid interface

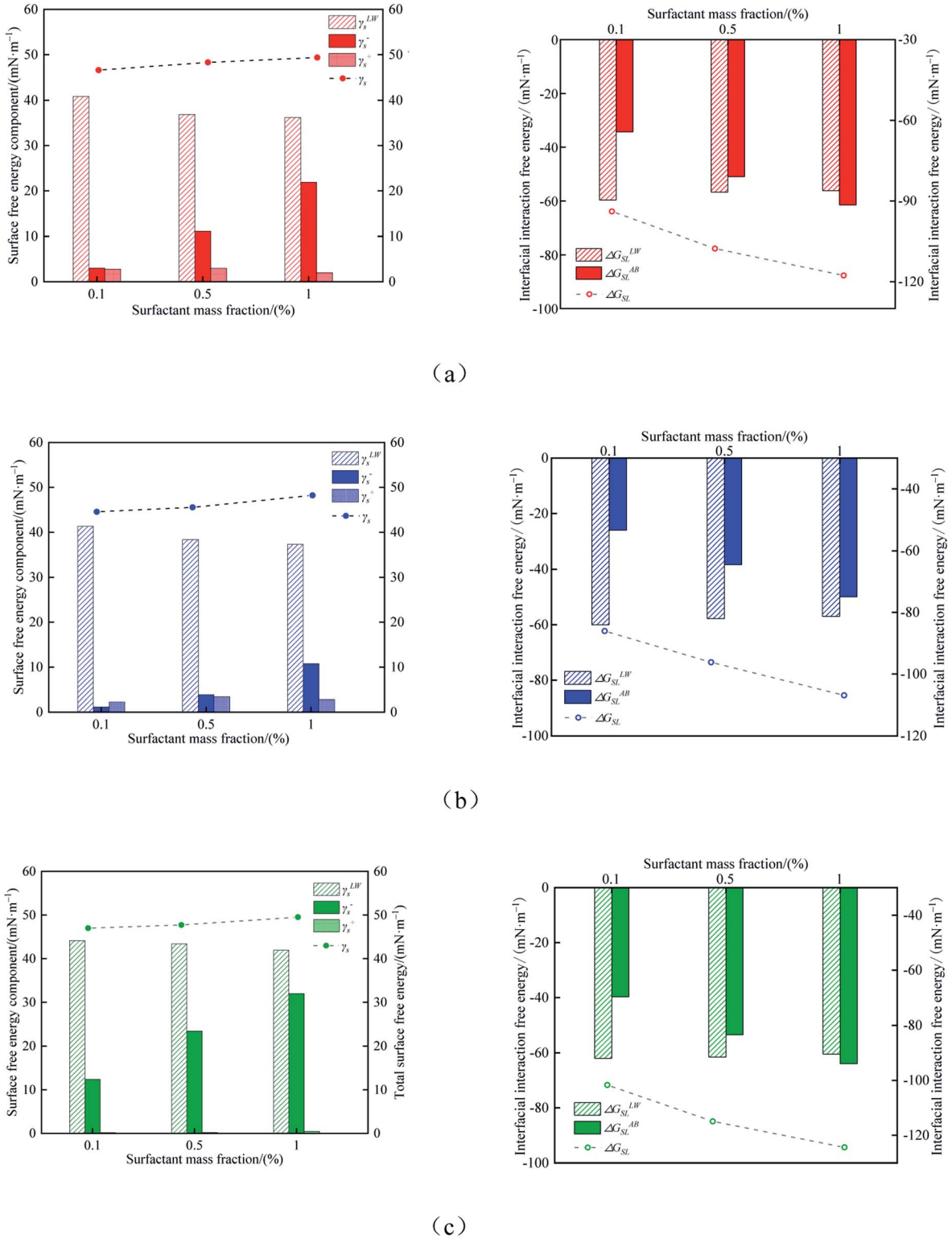

Fig. 5 Calculation results of surface free energy and interface interaction energy. (a) SDBS, (b) JFC, (c) Triton X-100.

interaction free energy ΔG_{sl}^{LW-AB} includes Lifshitz–van der Waals (LW) interaction free energy ΔG_{sl}^{LW} and Lewis acid–base (AB) interaction free energy ΔG_{sl}^{AB}, as shown in formula (7), formula (8) and formula (9):[30,31]

$$\Delta G_{sl}^{LW} = -2\sqrt{\gamma_s^{LW}\gamma_s^{LW}} \quad (7)$$

$$\Delta G_{sl}^{AB} = -2\sqrt{\gamma_s^{+}\gamma_l^{-}} - 2\sqrt{\gamma_s^{-}\gamma_l^{+}} \quad (8)$$

$$\Delta G_{sl}^{LW-AB} = \Delta G_{sl}^{LW} + \Delta G_{sl}^{AB} = -2\sqrt{\gamma_s^{LW}\gamma_l^{LW}} - 2\sqrt{\gamma_s^{+}\gamma_l^{-}} - 2\sqrt{\gamma_s^{-}\gamma_l^{+}} \quad (9)$$

Three kinds of test liquids (deionized water, formamide, and diiodomethane) were used to determine the contact angle. The physical parameters of the test liquid (analytically pure) are listed in Table 3.

The calculated results of surface free energy of raw coal without surfactant treatment are shown in Table 4.

The calculated surface free energy of raw coal without surfactant treatment is 44.51 mN m^{-1}. The surface free energy of raw coal without treatment is low and its hydrophilicity is poor. The surface free energy of coal is mainly dispersive composition, and the Lewis acid–base composition is very low, which indicates that hydrogen bonding seldom occurs on the surface of raw coal.

The calculated results of surface free energy and solid–liquid interface interaction energy of coal samples modified by three surfactants are shown in Fig. 5. The surface free energy of the coal modified by surfactants increases to varying degrees. The surface free energy increases with the increase in surfactant concentration of 0.1 wt%, 0.5 wt% and 1.0 wt%. It can be clearly seen that the surface free energy and Lewis acid–base interaction of coal are increased, which indicates that the probability of hydrogen bond formation on the surface of the coal modified by surfactants is greatly increased. After 1.0 wt% Triton X-100 modification, the surface free energy of the coal sample increases the most, which is 49.52 mN m^{-1}, and Lewis acid–base interaction is the largest, in which the proportion of γ_s^- is the highest. The adsorption of the surfactant greatly increases the probability of hydrogen bonding between the coal surface and water, and improves the wettability of coal. The difference in the modification effect of different kinds of surfactants is also reflected in the composition of surface free energy. The results indicate that the non-polar van der Waals of coal samples modified by the three surfactants has little difference, but the Lewis acid–base interaction has more difference. This indicates that the ability of hydrogen bonding between the hydrophilic end of the surfactant adsorbed on the coal surface and water molecules will affect the wettability of coal samples.

The results supra certify the strong modification dependence on the surfactant type. The three surfactants have various hydrophilic and hydrophobic groups and, therefore, diverse molecular structures, ultimately differentiating the modification effects. Accordingly, the molecular dynamics simulation approach is invoked to explore the surfactant adsorption mechanism at the molecular level.

Molecular dynamics simulation

To microscopically study the adsorption behavior of disparate surfactants on the coal surface, molecular dynamics simulation was carried out using the Material Studio software. There are many macromolecular models of coals, such as Fuchs model[32,33] modified in 1957, which has a honeycomb-like condensed aromatic ring but a low accuracy. The Given model[34] proposed in 1960 rationalizes the naphthalene rings as interconnected by aliphatic rings but not considers the sulfur-containing structure and ether bonds. The Honda model floated by Honda[35] first embraced both the organic small molecular compounds and multifarious oxygen-containing functional groups in the coal structure, but still not reckon with the sulfur and nitrogen structures. According to the coalification degree and the main surface functional groups of coals obtained by FT-IR spectroscopy, a more comprehensive and reasonable Wiser model[36] was postulated to stimulate the coal macromolecular model (Fig. 6). The model takes into account not only phenol, aryl ether, ring

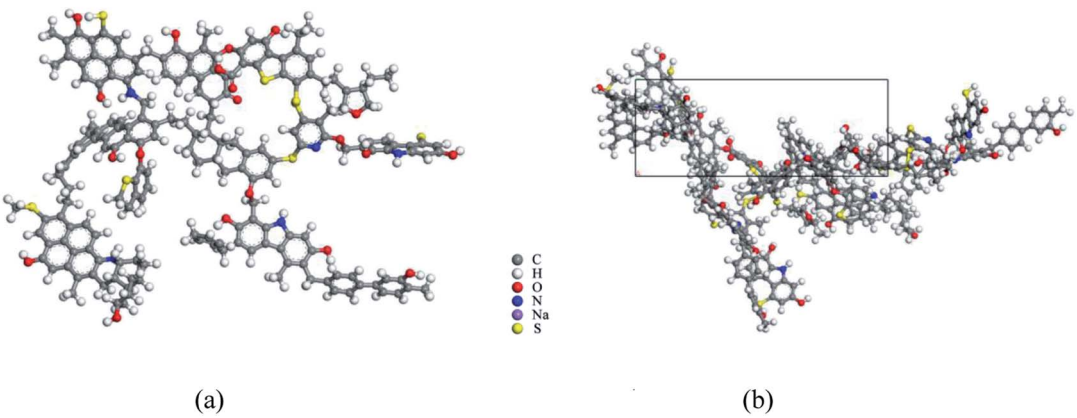

Fig. 6 Single coal molecule and crystal cell structure. (a) Wiser model after structure optimization, (b) periodic cell structure of two coal molecules.

structure containing oxygen, nitrogen and sulfur, but also the unstable structure like alcohol hydroxyl, amino group, and carboxyl group, which is suitable for high volatile bituminous coal.

Three surfactant molecules and a Wiser macromolecular model were first built and optimized using force module under the COMPASS force field. Amorphous cell module was employed to construct the periodic cell structure of 2 Wiser coal

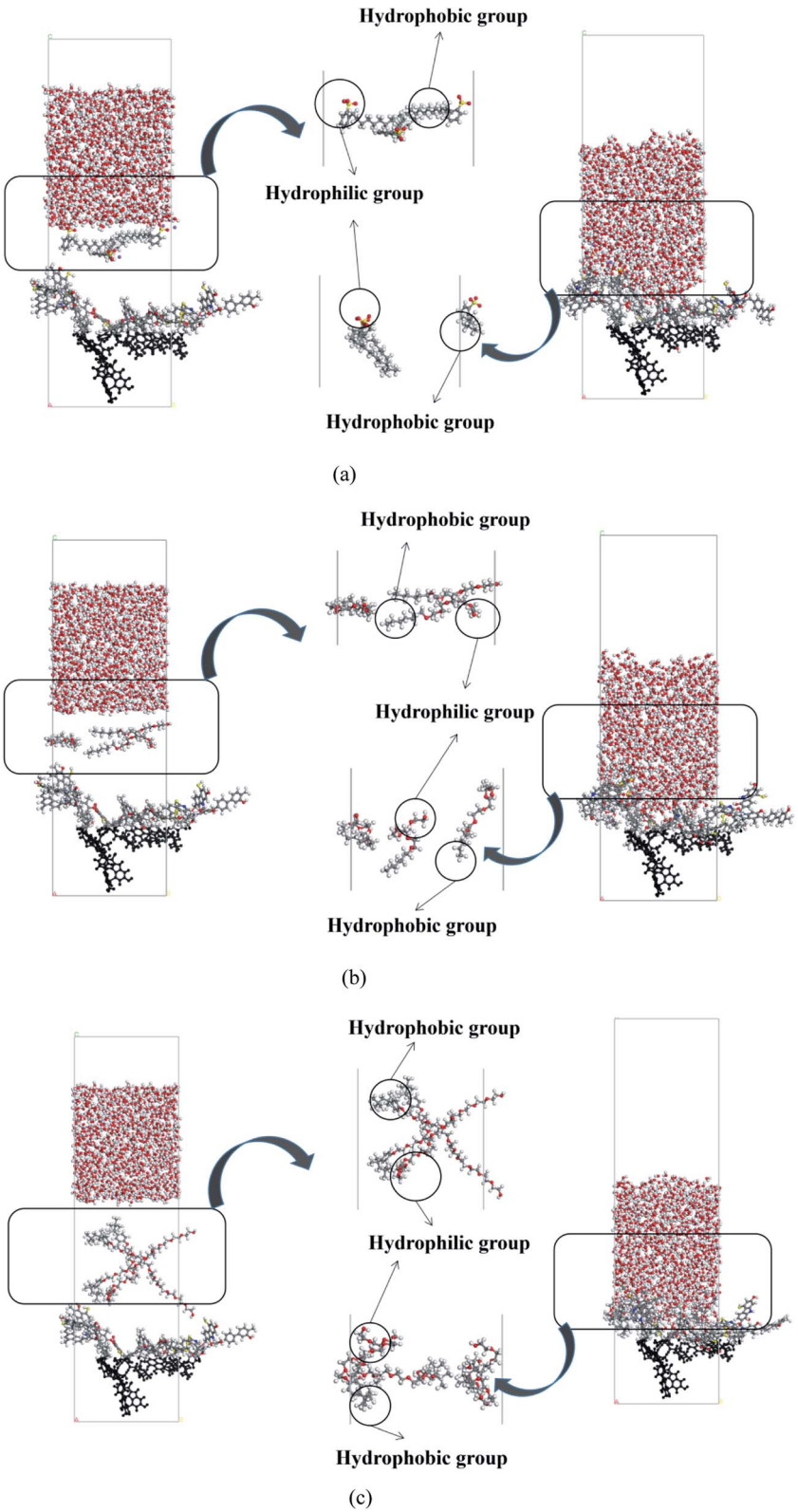

Fig. 7 Adsorption configuration of water/surfactant/coal. (a) Coal–SDBS, (b) coal–JFC, (c) coal–Triton X-100.

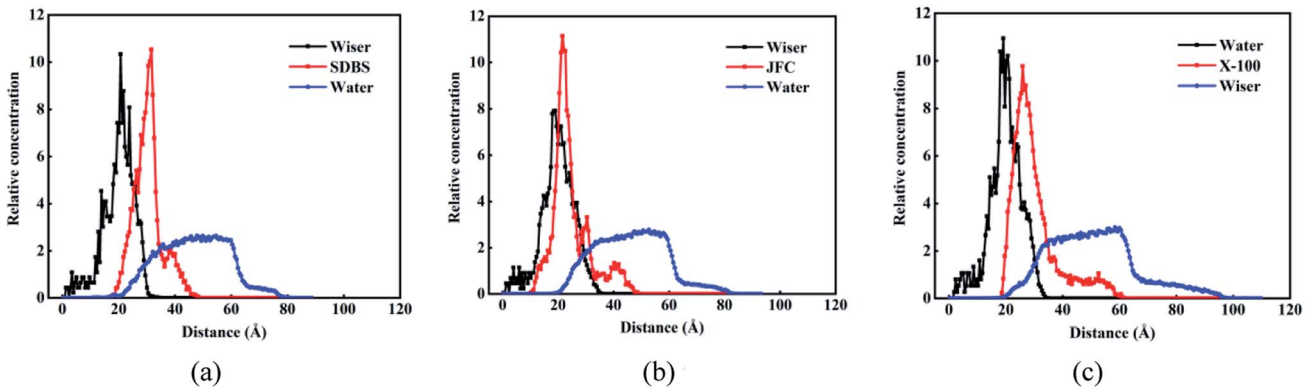

Fig. 8 Relative concentration distribution. (a) Coal–SDBS, (b) coal–JFC, (c) coal–Triton X-100.

molecules, 1000 water molecules and 3 surfactant molecules. Three different water/surfactant/coal 3-phase systems were established with a build layer tool. To reduce the calculation cost, 2/3 of the coal molecule was fixed and a vacuum layer of 10 Å was set above the coal molecule to eliminate the influence of the periodic structure. The geometry of the system was optimized to abrogate the unreasonable overlap between atoms. The canonical ensemble (*NVT*) was selected in the Forcite module and the temperature control method is Nosé thermostat. The dynamic simulation of the system under the COMPASS force field was carried out at a time step of 1 fs under 298 K. The electrostatic interaction and van der Waals action were calculated by the Ewald addition and atom-based methods, respectively. An operation time of 200 ps was mandated for the inappreciable temperature and energy fluctuation to strike an equilibrium, and hence, all systems were simulated for 200 ps. In order to ensure the repeatability of the simulation, the simulation is repeated three times.

The initial and equilibrium states of the three water/surfactant/coal adsorption models are shown in Fig. 7. The addition of surfactant and water molecules into the coal model can destroy the system's thermodynamic equilibrium due to the interaction between surfactant molecules and coal macromolecules. The hydrophobic group of surfactants was adsorbed on the coal surface, and the hydrophilic group was tilted to the side of water molecules to reach a new equilibrium state. In the SDBS adsorption model, the hydrophobic groups of surfactant molecules were grafted on hydrophobic groups of the coal surface to form a directional arrangement of hydrophilic groups pointing towards the water phase, shifting surface property from hydrophobicity to hydrophilicity. Since the nonionic surfactants (JFC, Triton X-100) could not be dissociated into the ionic state in water, the hydrophobic groups of surfactants tend to adsorb on the coal surface *via* van der Waals force. The hydrophilic chain of Triton X-100 nonionic surfactants contains 10 ethylene oxide units, which are connected to the aromatic ring through branched chain hydrocarbon chain. The longer molecular chains cross to generate an adsorption layer, and the hydrophilic group faces the water phase, thus changing the coal surface wettability.

Fig. 8 shows the relative concentration distribution of three kinds of surfactant adsorption configuration. The coal molecules are partly fixed, so the surfactant and water molecules only contact with the coal surface, and the coal distribution is basically unchanged. The distribution range of SDBS, JFC and Triton X-100 were 20–45 Å, 10–50 Å and 20–60 Å, respectively. The final adsorption configuration of the three systems suggests that SDBS has a shorter molecular chain and forms the thinnest adsorption layer. Other two nonionic surfactants possess longer molecular chains and a wider concentration distribution range. Triton X-100 possesses the closest surface adsorption conformation to the lying flat and thus the largest coverage on coal surfaces.

To compare the attraction of surfactants to water molecules, the number of hydrogen bonds formed between surfactants and water molecules was counted.

As shown in Fig. 9, SDBS molecules rely on the oxygen atom in the sulfate radical to form hydrogen bonds with the hydrogen atom of water molecules, and the number of hydrogen bonds is 12. For JFC and Triton X-100 molecules, the oxygen atom in hydroxyl groups at the molecular chain end and the oxygen atom in the ether bond can interplay with the hydrogen atom of water molecules into hydrogen bonds, whose number is 8 and 15, respectively, greatest in three surfactants, so providing most sites available to the water molecule. The Triton X-100 molecule adsorption layer on coal surfaces can shield the hydrophobic groups of coal molecules, and the hydrophilic end can attract more water molecules, thus provoking the exceptional modification effect. This is consistent with the results of contact angle test.

The adsorption of surfactants on the coal surface affects the structure of water phase and the movement of water molecules. The mean square displacement (MSD) can be used to determine the effect of surfactants on the aggregation of water molecules. The calculation formula is as follows:

$$\mathrm{MSD} = \frac{1}{N}\sum_{i=1}^{N}[r_i(t) - r_i(0)]^2 \quad (10)$$

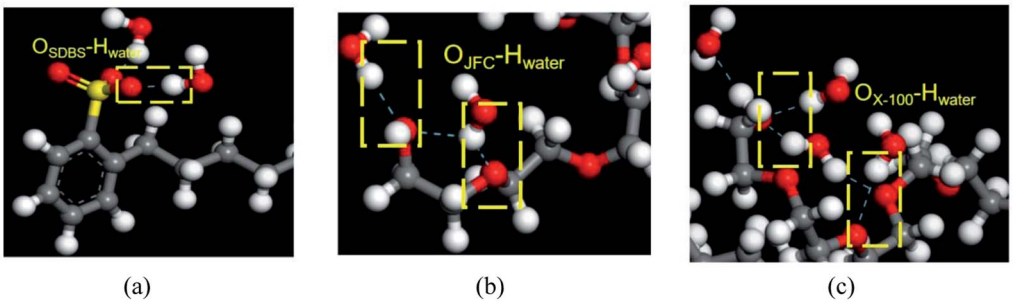

Fig. 9 Types of hydrogen bonds formed between three surfactants and water molecules. (a) SDBS, (b) JFC, (c) Triton X-100.

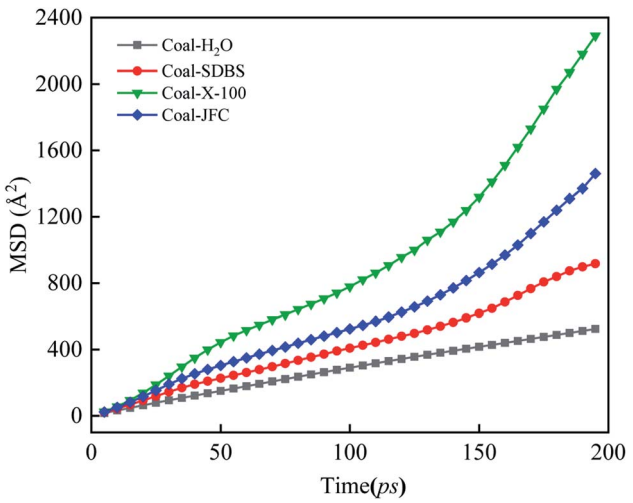

Fig. 10 Mean square displacement of water molecule.

According to the Einstein equation,[37] the diffusion coefficient (D) of the water molecule can be obtained as follows:

$$D = \frac{1}{6N}\lim_{t\to\infty}\frac{\mathrm{d}}{\mathrm{d}t}\sum_{i=1}^{N}[r_i(t) - r_i(0)]^2 \qquad (11)$$

For comparison, we constructed a model with only water and coal. The MSD curves of water molecules with four adsorption configurations are sketched in Fig. 10. Overall, the slope of MSD of water molecules in the surfactant-containing systems balloons compared with the surfactant counterpart. The diffusion coefficient of the water molecule is 0.44×10^{-5} cm^2 s^{-1} in the coal water system without surfactants. The MSD slope of the Triton X-100 system is the largest, and the water molecular diffusion coefficient is 1.78×10^{-5} cm^2 s^{-1}. The surfactant introduction augments the water molecule diffusion, the interaction between water and coal, and thus, the coal hydrophilicity.

The interaction strength can be evaluated by calculating the interaction energy of the system. The lower energy and greater negative interaction energy could spur the steadier adsorption.[38] However, the interaction energy of the simulation system only represents the interaction strength between the surfactant and coal surface, which is not equal to the thermodynamic adsorption energy.[39] The interaction energy is defined as the difference between the energy of the complex and the sum of the energies of the monomers constituting the complex. The interaction energy between surfactant and coal was calculated as follows:

$$E_{\mathrm{int}} = (E_{\mathrm{t}} - E_{\mathrm{s}} - E_{\mathrm{c+w}} - E_{\mathrm{c}} - E_{w+\mathrm{s}} + E_{\mathrm{w}} + E_{\mathrm{s+c}})/2 \qquad (12)$$

where E_{int} is the interaction energy of the system, E_{t} is the total energy of the system, E_{c}, E_{s} and E_{w} are the energies of coal surface, surfactant, and water respectively, and $E_{\mathrm{w+c}}$, $E_{\mathrm{s+c}}$ and $E_{\mathrm{s+w}}$ are the total energies of water and coal, surfactant and coal, surfactant and water, respectively (Table 5).

The results indicate that the interaction energies of the three surfactants are all negative, explaining the spontaneous adsorption process. Among the three adsorption systems, the interaction energy of Triton X-100 adsorption model is the largest, demystifying a very stable adsorption between coal and water molecules. This notable difference in interaction energies was endowed by the inherent structural disparity of surfactants JFC and Triton X-100 as typical nonionic surfactants yet have different hydrophobic groups. The hydrophobic groups of JFC are hydrocarbon chain structures and can interact with the hydrophobic groups on the coal surface mainly *via* weak van der Waals force. The hydrophobic group of Triton X-100 is a branched chain structure containing a benzene ring, and the

Table 5 Calculation results of interaction energy

System	E_{t} kJ mol^{-1}	E_{w} kJ mol^{-1}	$E_{\mathrm{s+c}}$ kJ mol^{-1}	E_{c} kJ mol^{-1}	$E_{\mathrm{s+w}}$ kJ mol^{-1}	E_{s} kJ mol^{-1}	$E_{\mathrm{w+c}}$ kJ mol^{-1}	E_{int} kJ mol^{-1}
SDBS	−5469.21	−7601.61	2828.94	3161.39	−8357.41	−264.55	−4645.51	−67.90
JFC	−4936.45	−7806.56	3156.99	3152.63	−7765.08	111.95	−4870.34	−107.59
X-100	−4959.28	−7814.83	3161.21	3117.81	−7769.15	188.30	−4858.37	−145.75

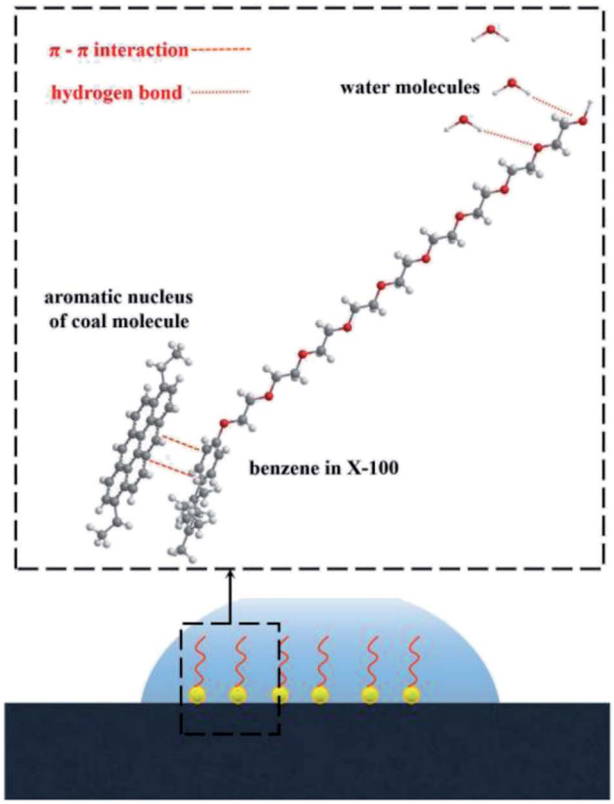

Fig. 11 Schematic diagram of the interaction of Triton X-100 molecule with coal molecule and water molecule (the gray atoms are carbon atoms, the white atoms are hydrogen atoms, and the red atoms are oxygen atoms).

main body of the coal molecule is the aromatic structure. A large number of aromatic rings in the coal molecule will form the strong π–π interaction with the benzene ring in Triton X-100, rendering steadier the adsorption between the surfactant molecule and coal.[40,41] Compared with the straight chain JFC, the branched chain structure of the hydrophobic end of Triton X-100 also makes it have higher activity.[42] The adsorption configuration of SDBS is more like an upright state, with the hydrophilic group towards the water molecule and the benzene ring far away from the coal molecule. Consequently, no π–π interaction between SDBS and coal molecule turns up, inducing the small interaction energy with the coal molecule.

In terms of the hydrogen bond between the surfactant and the water molecule, the number of hydrogen bonds is less for the JFC system than for the Triton X-100 and SDBS systems, and the as-formed adsorption layer has much weaker attraction to water molecules. On the whole, the interaction landscape between the surfactant, water and coal explicitly corroborates the striking modification effect of the Triton X-100 molecule upon the coal hydrophilicity, as pictured in Fig. 11.

Conclusions

(1) In this study, the contact angle tests proved that surfactants can notably tune the coal wettability. The obvious surfactant type and concentration effects were found. A higher concentration, a better promotion effect. The optimal nonionic Triton X-100 molecule can cause the contact angle to drop by 47%. The surface free energy of the coal sample modified by the surfactant increases, the proportion of polar Lewis acid–base composition increases, and the probability of hydrogen bonding on coal surface increases greatly.

(2) Molecular dynamics simulation was leveraged to expound the experimental phenomenon. The surfactant molecules can adsorb onto the coal surface *via* hydrophobic groups and the hydrophilic groups face the water phase, which alters the interaction between the coal surface and water. Particularly, Triton X-100 has the largest interaction energy with coal and the most stable adsorption more hydrogen bonds with coal molecules, thus improving the coal surface hydrophilicity, expediting the movement of water molecules on the coal surface, and increasing the diffusion coefficient.

(3) The experimental results and adsorption simulation explicitly corroborates that the benzene ring in the Triton X-100 molecule can form stable π–π interactions with the hydrophobic aromatic ring structure in the coal molecule, while its hydrophilic group can form hydrogen bonds with the water molecule to thus reinforce the coal surface hydrophilicity and the water adsorption on coal surfaces.

In summary, this unique interaction of the hydrophobic structure of Triton X-100 and the aromatic structure of coal molecules made the adsorption on the coal surface strong and stable, and the hydrophilic end of Triton X-100's excellent ability to form a large number of hydrogen bonds with water molecules unveils the outstanding ability of Triton X-100 to manipulate the coal surface hydrophilicity, offering invaluable guidance for pragmatic dust control.

Conflicts of interest

There are no conflicts to declare.

Acknowledgements

This work was financially supported by National Natural Science Foundation of China (U2013603; 52004167); the Key Research and Development Program of Sichuan Science and Technology Department (2019YFS0513); the Applied Basic Research Programs of Sichuan Province (2019YJ0136, 2021YJ0411).

References

1 J. Fu and Y. Cheng, Situation of coal and gas outburst in China and control countermeasures, *J. Min. Saf. Eng.*, 2007, **24**(3), 253–259.
2 H. Xie, M. Gao, Ru Zhang, G. Peng, W. Wang and A. Li, Study on the Mechanical Properties and Mechanical Response of Coal Mining at 1000 m or Deeper, *Rock Mechanics and Rock Engineering*, 2019, **52**(5), 1475–1490.
3 H. Xie, J. Xie, M. Gao, Ru Zhang, H. Zhou, F. Gao and Z. Zhang, Theoretical and experimental validation of

mining-enhanced permeability for simultaneous exploitation of coal and gas, *Environ. Earth Sci.*, 2015, **73**(10), 5951–5962.

4 W. Xiujun, M. Gao, Y. Lv, X. Shi, H. Gao and H. Zhou, Evolution of a mining induced fracture network in the overburden strata of an inclined coal seam, *Int. J. Min. Sci. Technol.*, 2012, **22**(06), 775–779.

5 J. Zhang, H. Li, Y. Liu, *et al.*, Micro-wetting characteristics of coal dust in Pingdingshan mining area and preliminary study on the development of dust suppressant, *J. China Coal Soc.*, 2021, **46**(3), 812–825.

6 B. Kong, E. Wang and Z. Li, The effect of high temperature environment on rock properties-an example of electromagnetic radiation characterization, *Environ. Sci. Pollut. Res.*, 2018, **25**(29), 29104–29114.

7 G. Xu, Y. Chen, J. Eksteen, *et al.*, Surfactant-aided coal dust suppression: a review of evaluation methods and influencing factor, *Sci. Total Environ.*, 2018, **639**(22), 1060–1076.

8 Y. Chen, G. Xu and B. Albijanic, Evaluation of SDBS surfactant on coal wetting performance with static methods: Preliminary laboratory tests, *Energy Sources, Part A*, 2017, **39**(23), 2140–2150.

9 R. J. Crawford and D. E. Mainwaring, The influence of surfactant adsorption on the surface characterisation of Australian coals, *Fuel*, 2001, **80**(3), 313–320.

10 S. Li, L. Gao, J. Wang, G. Rong and Y. Cao, Enhancement of floatability of low-rank coal using oxidized paraffin soap, *RSC Adv.*, 2020, **10**(26), 15098–15106.

11 V. K. Kollipara, Y. P. Chugh and K. Mondal, Physical, mineralogical and wetting characteristics of dusts from Interior Basin coal mines, *Int. J. Coal Geol.*, 2014, **127**, 75–87.

12 J. Kang, *Experimental study on modification of Anthracite and Its Effect on Adsorption and Wettability*, Taiyuan University of Technology, 2018.

13 G. Ni, Q. Sun, X. Meng, H. Wang, Y. Xu, W. Cheng and G. Wang, Effect of NaCl-SDS compound solution on the wettability and functional groups of coal, *Fuel*, 2019, 257.

14 B. Nie, X. He, E. Wang, *et al.*, Micro-Mechanism of Coal Adsorbing Water, *J. China Univ. Min. Technol.*, 2004, **33**(4), 379–383.

15 S. Paria and K. C. Khilar, A review on experimental studies of surfactant adsorption at the hydrophilic solid-water interface, *Adv. Colloid Interface Sci.*, 2004, **110**(3), 75–95.

16 Y. Xia, R. Zhang, Y. Xing and X. Gui, Improving the adsorption of oily collector on the surface of low-rank coal during flotation using a cationic surfactant: An experimental and molecular dynamics simulation study, *Fuel*, 2019, 235.

17 X. You, H. Meng, W. Zhang, H. Wei, X. Lyu, Q. Q. He and L. Li, Molecular dynamics simulations of nonylphenol ethoxylate on the Hatcher model of subbituminous coal surface, *Powder Technol.*, 2018, 332.

18 M. Yuan, N. Wen, W. Zhou, *et al.*, Determining the effect of the non-ionic surfactant AEO 9 on lignite adsorption and wetting *via* molecular dynamics (MD) simulation and experiment comparisons, *Fuel*, 2020, 278.

19 Y. Zhou, B. Albijanic, Y. Wang and J. Yang, Characterizing surface properties of oxidized coal using FTIR and contact angle measurements, *Energy Sources, Part A*, 2018, **40**(12), 1559–1564.

20 Y. Lu, F. Li, X. Jiang, Y. Zhao, G. Zhao and C. Yuan, Construction of a molecular structure model of mild-oxidized Chinese lignite using Gaussian09 based on data from FTIR, solid state 13C-NMR, *J. Mol. Model.*, 2018, **24**(6).

21 H. I. Petersen, P. Rosenberg and H. P. Nytoft, Oxygen groups in coals and alginite-rich kerogen revisited, *Int. J. Coal Geol.*, 2008, **74**(2), 93–113.

22 J. Zhou, *Study on The Distribution of O-containing Functional Groups in Low rank coals and Its Removal Methods*, China University of Mining & Technology, Beijing, 2014.

23 X. Wang, S. Yuan and B. Jiang, Experimental investigation of the wetting ability of surfactants to coals dust based on physical chemistry characteristics of the different coal samples, *Adv. Powder Technol.*, 2019, **30**(8), 1696–1708.

24 T. Young, An Essay on the Cohesion of Fluids, *Philos. Trans. R. Soc. London*, 1805, **95**, 65–87.

25 D. Y. Kwok and A. W. Neumann, Contact angle interpretation: re-evaluation of existing contact angle data, *Colloids Surf., A*, 2000, **161**(1), 49–62.

26 C. J. Van-Oss, M. K. Chaudhury and R. J. Good, Mechanism of partition in aqueous media, *Sep. Sci. Technol.*, 1987, **22**(6), 1515–1526.

27 C. J. Van-Oss, R. J. Good and M. K. Chaudhury, Estimation of the polar surface tension parameters of glycerol and formamide, for use in contact angle measurements on polar solids, *J. Dispersion Sci. Technol.*, 1990, **11**(1), 75–81.

28 C. J. Van-Oss, R. J. Good and M. K. Chaudhury, The role of van der Waals forces and hydrogen bonds in "hydrophobic interactions" between biopolymers and low energy surfaces, *J. Colloid Interface Sci.*, 1986, **111**, 378–390.

29 A. Voelkel, B. Strzemiecka, K. Adamska and K. Milczewska, Inverse gas chromatography as a source of physiochemical data, *J. Chromatogr. A*, 2009, **1216**, 1551–1566.

30 M. Espinosa-Jimenez, A. Ontiveros-Ortega and E. Gimenez-Martin, Surface energetics of the adsorption process of a cationic dye on leacril fabrics, *J. Colloid Interface Sci.*, 1997, **194**(2), 419–426.

31 M. Espinosa-Jimenez, E. Gimenez-Martin and A. Ontiveros-Ortega, Effect of tannic acid on the ζ potential, sorption and surface free energy in the process of dyeing of leacril with a cationic dye, *J. Colloid Interface Sci.*, 1998, **207**(1), 170–179.

32 P. Meshram, *et al.*, Demineralization of low grade coal-A review, *Renewable Sustainable Energy Rev.*, 2015, **41**, 745–761.

33 J. P. Mathews and A. L. Chaffee, The molecular representations of coal-A review, *Fuel*, 2012, **96**, 1–14.

34 P. H. Given, The distribution of hydrogen in coals and its relation to coal structure, *Fuel*, 1960, **39**(2), 147.

35 X. Meng, *et al.*, Construction of a macromolecular structural model of Chinese lignite and analysis of its low-temperature oxidation behavior, *Chin. J. Chem. Eng.*, 2017, **25**(9), 1314–1321.

36 W. H. Wiser, *Division of Fuel Chemistry*, 1975, **20**(1), 122preprints.
37 A. R. Zolghadr, M. H. Ghatee and A. Zolghadr, Adsorption and orientation of ionic liquids and ionic surfactants at heptane/water interface, *J. Phys. Chem. C*, 2014, **118**(34), 19889–19903.
38 I. Moncayo-Riascos, J. D. León and B. A. Hoyos, Molecular dynamics methodology for the evaluation of the chemical alteration of wettability with organosilanes, *Energy Fuels*, 2016, **30**(5), 3605–3614.
39 B. Rai, P. Sathish, J. Tanwar, K. S. Pradip Moon and D. W. Fyerstenau, A molecular dynamics study of the interaction of oleate and dodecylammonium chloride surfactants with complex aluminosilicate minerals, *J. Colloid Interface Sci.*, 2011, **362**(2), 510–516.
40 L. Zhu, Yi Liu, X. Peng, *et al.*, Noble-Metal-Free CdS Nanoparticle-Coated Graphene Oxide Nanosheets Favoring Electron Transfer for Efficient Photoreduction of CO_2, *ACS Appl. Mater. Interfaces*, 2020, **12**(11), 12892–12900.
41 R. Qi, Y. Zhu, L. Han, *et al.*, Rectangular Platelet Micelles with Controlled Aspect Ratio by Hierarchical Self-Assembly of Poly (3-hexylthiophene)-*b*-poly (ethylene glycol), *Macromolecules*, 2020, **53**(15), 6555–6565.
42 D. Zhang, *The Dynamic Adsorption Spreading of Typical Non-ionic Surfactants and Wetting Mechanism of Coal Dust*, Taiyuan University of Technology, 2016.